

Measurement of electron correlations in Li_xCoO_2 ($x=0.0-0.35$) using ^{59}Co nuclear magnetic resonance and nuclear quadrupole resonance techniques

S. Kawasaki,¹ T. Motohashi,^{2,3} K. Shimada,¹ T. Ono,^{2,4} R. Kanno,⁴ M. Karppinen,^{2,5} H. Yamauchi,^{2,4,5} and Guo-qing Zheng¹

¹*Department of Physics, Okayama University, Okayama 700-8530, Japan*

²*Materials and Structures Laboratory, Tokyo Institute of Technology, Yokohama 226-8503, Japan*

³*Graduate School of Engineering, Hokkaido University, N13 W8, Kita-ku, Sapporo 060-8628, Japan*

⁴*Interdisciplinary Graduate School of Science and Engineering, Tokyo Institute of Technology, Yokohama 226-8502, Japan*

⁵*Department of Chemistry, Laboratory of Inorganic Chemistry, Helsinki University of Technology, FI-02015 TKK, Finland*

(Received 11 February 2009; revised manuscript received 23 April 2009; published 24 June 2009)

CoO_2 is the parent compound for the superconductor $\text{Na}_x\text{CoO}_2 \cdot 1.3\text{H}_2\text{O}$ and was widely believed to be a Mott insulator. We performed ^{59}Co nuclear magnetic resonance and nuclear quadrupole resonance studies on Li_xCoO_2 ($x=0.35, 0.25, 0.12$, and 0.0) to uncover the electronic state and spin correlations in this series of compounds which was recently obtained through electrochemical deintercalation of Li from pristine LiCoO_2 . We find that although the antiferromagnetic spin correlations systematically increase with decreasing Li content (x), the end member, CoO_2 , is a noncorrelated metal that well satisfies the Korringa relation for a Fermi liquid. Thus, CoO_2 is not simply located at the limit of $x \rightarrow 0$ for $A_x\text{CoO}_2$ ($A=\text{Li}, \text{Na}$) compounds. The disappearance of the electron correlations in CoO_2 is due to the three dimensionality of the compound which is in contrast to the highly two-dimensional structure of $A_x\text{CoO}_2$.

DOI: 10.1103/PhysRevB.79.220514

PACS number(s): 74.25.Jb, 74.25.Nf, 74.70.-b

Electronic correlations and superconductivity in transition-metal oxides have been a main focus in condensed matter physics since the discovery of high-transition-temperature (T_c) superconductivity in copper oxides. The hydrated cobalt-oxide superconductor $\text{Na}_x\text{CoO}_2 \cdot 1.3\text{H}_2\text{O}$ has intensified the research interest in the past few years.¹ This compound bears similarities to the high- T_c copper oxides in that it has a quasi-two-dimensional crystal structure and contains a transition-metal element that carries a spin of $\frac{1}{2}$. Indeed, nuclear quadrupole resonance (NQR) measurements on $\text{Na}_x\text{CoO}_2 \cdot 1.3\text{H}_2\text{O}$ have found T^3 variation below T_c in the spin-lattice relaxation rate $1/T_1$, which is a strong indication of existence of line nodes in the superconducting gap function.²⁻⁴ Precise measurements of the Knight shift in a high quality single crystal reveal that the spin susceptibility decreases below T_c along both a - and c -axis directions, which indicates that the Cooper pairs are in the spin-singlet state.⁵ Thus, the superconductivity in $\text{Na}_x\text{CoO}_2 \cdot 1.3\text{H}_2\text{O}$ appears to be of d -wave symmetry, as in the case of high- T_c copper oxides. It has also been found that antiferromagnetic spin correlations are present in the superconducting cobaltates, though being much weaker than those in the cuprates.^{2,3} The correlations are anisotropic in the spin space,⁶ which is different from the cuprate case.

Then, a natural question is how to model the cobalt oxides. Many authors applied the so-called t - J model that had been widely used to describe the cuprates.⁷⁻⁹ In these theories, one virtually starts from CoO_2 in which Co is in the Co^{4+} state and there is one electron ($s=1/2$) in the lowest level (a_{1g} orbital). Upon adding Na, one dopes electrons into the a_{1g} orbital and creates a Co^{3+} ($s=0$) state. In such a scenario, one may be in a situation of dealing with a doped Mott insulator, as in the cuprates case.^{7,8,10} Therefore, it is important to synthesize the CoO_2 phase and to reveal its electronic ground state. Unfortunately, it has been chemically difficult to obtain pure phase of CoO_2 , or even Na_xCoO_2 with

$x \leq 0.25$, though some efforts have been reported.¹¹⁻¹³

In this Rapid Communication, we report ^{59}Co -NMR and NQR studies to uncover the electronic state and spin correlations in Li-deficient phases, Li_xCoO_2 ($x=0.35, 0.25$, and 0.12), and the CoO_2 phase. Although the antiferromagnetic spin correlation increases with reducing Li content (x), the end member, CoO_2 , is found to be a noncorrelated metal that well satisfies the Korringa relation for a Fermi liquid. The result obtained from our CoO_2 sample is different from the one reported earlier¹¹ in both the temperature (T) dependence and the magnitude of the $1/T_1$. It turns out that the earlier result corresponds to that of our $\text{Li}_{0.12}\text{CoO}_2$. We argue that, however, the disappearance of the electron correlations in pure CoO_2 is due to the three dimensionality of the compound which collapses from the highly two-dimensional structure of $A_x\text{CoO}_2$ ($A=\text{Li}, \text{Na}$) when Li is completely removed. The systematic evolutions of the electron correlations in Li_xCoO_2 ($x=0.35, 0.25$, and 0.12), as well as in $\text{Na}_x\text{CoO}_2 \cdot 1.3\text{H}_2\text{O}$ ($x=0.35, 0.33, 0.28$, and 0.25),³ are consistent with the theoretical postulation that $A_x\text{CoO}_2$ ($A=\text{Li}, \text{Na}$) with small x is near a magnetic instability.^{7,8}

Polycrystalline samples of Li_xCoO_2 ($x=0.35, 0.25$, and 0.12) and CoO_2 ($x=0.0$) were synthesized through electrochemical deintercalation of Li from pristine LiCoO_2 , as described elsewhere.^{14,15} Approximately 100 mg of single-phase LiCoO_2 (without additives) was electrochemically oxidized with a constant current of 0.1 mA in an airtight flat cell filled with a nonaqueous electrolyte. The Li content (or the amount of Li ions to be extracted, i.e., $1-x$) of each sample was precisely controlled by the reaction duration based on Faraday's law. Typically, a 100 mg LiCoO_2 pellet was charged for 178, 205, 241, and 274 h to obtain the $x=0.35, 0.25, 0.12$, and 0.0 (i.e., CoO_2) phases, respectively. As seen in Fig. 1, x-ray powder diffraction analysis evidenced that all the samples are of single phase with characteristic crystal structures typical for their Li compositions.

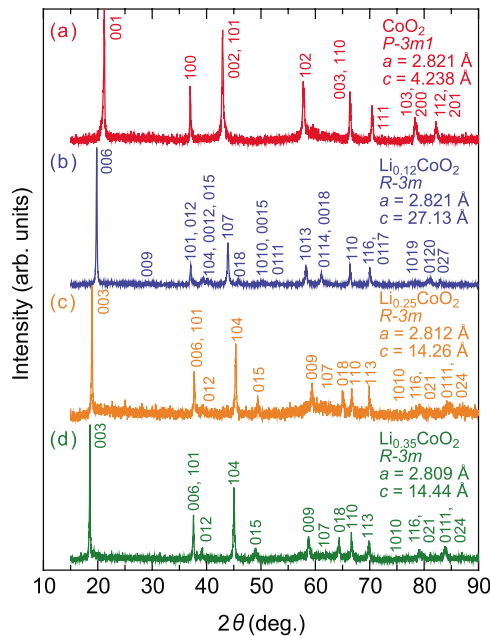


FIG. 1. (Color online) X-ray powder diffraction patterns for (a) CoO_2 , (b) $\text{Li}_{0.12}\text{CoO}_2$, (c) $\text{Li}_{0.25}\text{CoO}_2$, and (d) $\text{Li}_{0.35}\text{CoO}_2$ samples. For these samples, Rietveld refinement of the crystal structure was unsuccessful as the use of an airtight sample holder had significantly deteriorated the resolution of the diffraction patterns.

Sharp diffraction peaks throughout the XRD patterns demonstrate that our Li_xCoO_2 and CoO_2 samples are chemically homogenous with good crystallinity. The actual x values determined by inductively coupled plasma-atomic emission spectroscopy (ICP-AES) were in excellent agreement with the theoretical ones, indicating that the full amount of electricity due to the current was used for Li deintercalation from LiCoO_2 . Since high-valent cobalt oxides tend to experience chemical instability when exposed to atmospheric moisture,

sample handling and characterization were carefully made in an inert gas atmosphere. A part of the electrochemically treated samples (~ 70 mg) was encapsulated into a Pyrex ampule filled with Ar gas. NMR/NQR measurements were performed by using a phase-coherent spectrometer. The NQR measurements were performed at zero magnetic field. The NMR and NQR spectra were taken by changing the external magnetic field (H) at a fixed rf frequency of 71.1 MHz and by changing rf frequency and recording the spin-echo intensity step by step, respectively. The value of $1/T_1$ was extracted by fitting the nuclear magnetization obtained by recording the spin-echo intensity to the master equation.^{16,17}

Figure 2(a) shows a representative ^{59}Co -NMR spectrum for CoO_2 . The spectrum shows a typical randomly oriented powder pattern. Since ^{59}Co nucleus has nuclear spin $I=7/2$, an NMR spectrum has seven peaks due to the quadrupole interaction.¹⁸ As schematically shown by solid and dotted arrows in Fig. 2(a), the observed spectrum consists of two central peaks that originated from the anisotropy of the Knight shift along the ab -(K_{ab}) and c -(K_c) directions and each central peak is accompanied by six satellite peaks. The numerical calculation considering the quadrupole effect up to the second-order perturbation completely reproduced the experimental result [solid curve in Fig. 2(a)]. The clear peak structure attests the high quality of the sample. Thus, we are able to obtain the values of K_{ab} and K_c precisely from the NMR spectra. Figure 2(b) shows the ^{59}Co -NQR spectra for Li_xCoO_2 ($x=0.0, 0.12$, and 0.35) observed at zero magnetic field. As in $\text{Na}_x\text{CoO}_2 \cdot y\text{H}_2\text{O}$,^{2,3} three NQR transition lines arising from $I=7/2$ are clearly observed in Li_xCoO_2 . For $x=0.35$, satellite peaks are observed as indicated by the arrows in Fig. 2(b). It indicates that a secondary phase is present in this composition, although x-ray diffraction immediately after sample synthesis showed a single-phase pattern. Since these peaks increased in intensity as time elapsed (not shown), this is an extrinsic phase that arises after the x-ray diffraction analysis.

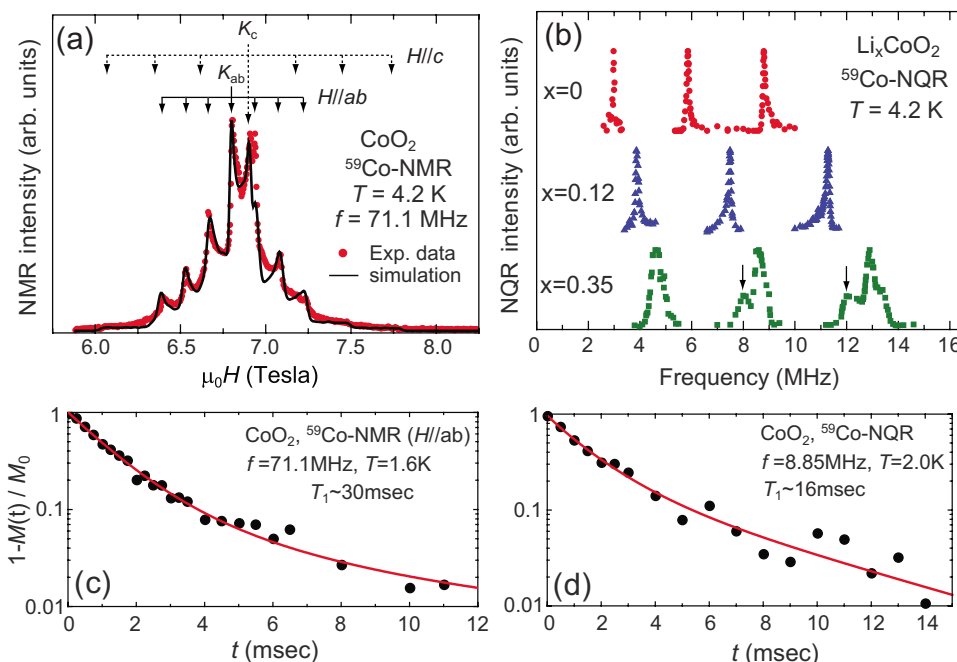


FIG. 2. (Color online) (a) ^{59}Co NMR spectrum for CoO_2 measured at $T=4.2$ K. The NMR frequency is 71.1 MHz. Solid and dotted arrows indicate the two sets of seven NMR peaks originated from anisotropy of the Knight shift, respectively. (b) NQR spectra for Li_xCoO_2 ($x=0.0, 0.12$, and 0.35) measured at $T=4.2$ K. Arrows indicate that extrinsic NQR peaks occurred due to aging (degradation). (c) and (d) are typical data sets of ^{59}Co nuclear recovery curves for CoO_2 obtained by NMR and NQR, respectively (see text).

TABLE I. NQR parameters for Li_xCoO_2 obtained at 4.2 K.

Sample	$^{59}\nu_Q$ (MHz)	η
CoO_2	2.93	0.05 ± 0.01
$\text{Li}_{0.12}\text{CoO}_2$	3.76	0.09 ± 0.01
$\text{Li}_{0.35}\text{CoO}_2$	4.32	0.10 ± 0.02

Figures 2(c) and 2(d) show typical data sets of ^{59}Co nuclear recovery curves to obtain T_1 by NMR and NQR, respectively. As drawn in solid curves in figures, they can be fitted by single component of theoretical curves^{16,17} even though the T_1 is measured in powdered sample. Compared to the early report in which the NMR spectrum did not show clear peak structure since it was a superposition of signals from different phases and T_1 is not of single component,¹¹ it is obvious that the present sample has much better quality, and the result represents, we believe, the intrinsic property of CoO_2 .

The NQR parameters are summarized in Table I. Here ν_Q and asymmetry parameter η are defined as $\nu_Q \equiv \nu_z = \frac{3}{2I(2I-1)\hbar} e^2 Q \frac{\partial^2 V}{\partial z^2}$ and $\eta = \frac{|\nu_x - \nu_y|}{\nu_z}$, with Q and $\frac{\partial^2 V}{\partial \alpha^2}$ ($\alpha = x, y, z$) being the nuclear quadrupole moment and the electric field gradient (EFG) at the position of the Co nucleus, respectively.¹⁸ Notably, ν_Q increases with increasing x . This assures electron doping by the increase in Li content. On the other hand, η is almost the same in $x=0.12$ and 0.35 but is substantially reduced in CoO_2 . This is because the CoO_2 phase crystallizes in a simple structure containing CoO_2 layers only (the so-called O1-type structure), while the crystal of Li_xCoO_2 consists of alternate stacking of Li_x and CoO_2 blocks.¹⁴

Figure 3(a) shows the T dependence of the Knight shift (K_{ab} and K_c) for three samples with different Li contents. As clearly seen in the figure, both K_{ab} and K_c of Li_xCoO_2 do not depend on temperature. Here, the Knight shift consists of contributions from the spin susceptibility, K_s , and from the orbital susceptibility (Van Vleck susceptibility), K_{orb} . $K = K_s + K_{orb}$, with K_{orb} being T independent but K_s being T dependent generally. $K_s(T)$ and K_{orb} are, respectively, related to the spin susceptibility χ_s and orbital susceptibility χ_{orb} as $K_s(T) = A_{hf}\chi_s(T)$ and $K_{orb} = A_{orb}\chi_{orb}$, where A_{hf} is the hyperfine coupling constant between the nuclear and the electron spins. The results show that the spin susceptibility in Li_xCoO_2 is T independent.

Figure 3(b) shows the T dependence of $1/T_1T$ measured by ^{59}Co NMR with $H \parallel ab$. Surprisingly, the $1/T_1T$ for CoO_2 is T independent. Together with the T -independent Knight shift in CoO_2 , the Korringa relation is satisfied as will be discussed later in more detail. This is a strong and the first evidence for a weakly correlated ground state of CoO_2 .

De Vaulx *et al.*¹¹ suggested that CoO_2 is a strongly correlated system on the basis of a small value of the characteristic temperature, T^* , below which the Korringa relation holds. However, as seen in Fig. 3(b) inset, we find that their result is similar to the result for our $\text{Li}_{0.12}\text{CoO}_2$ sample. As the authors acknowledged,¹¹ their sample contained a Li-rich phase as impurity. We suggest that the present results clarify the true electronic state of CoO_2 .

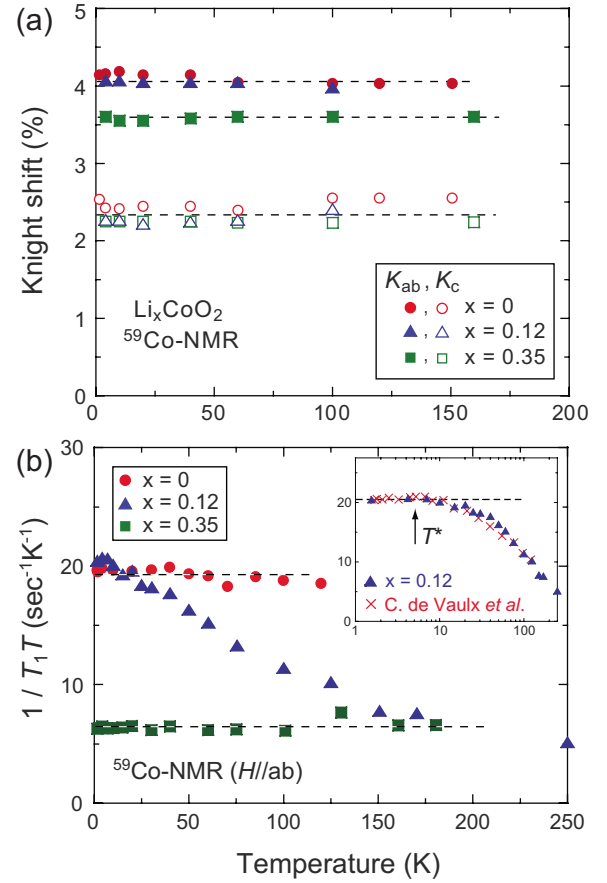


FIG. 3. (Color online) (a) T dependence of the Knight shift (K) for Li_xCoO_2 ($x=0.35, 0.12$, and 0.0) along the ab (solid symbols) and c axes (open symbols), respectively. Dotted lines indicate the relation of $K = \text{constant}$. (b) T dependence of ^{59}Co -NMR $1/T_1T$ for Li_xCoO_2 ($x=0.35, 0.12$, and 0.0) measured at the field along the ab axis. Inset shows the semilog plot of T dependence of ^{59}Co -NMR $1/T_1T$ for $\text{Li}_{0.12}\text{CoO}_2$ ($H \parallel ab$) along with the data referred from Ref. 11. Dotted lines indicate the relation of $1/T_1T = \text{constant}$. Arrow indicates T^* (see text).

We further measured T_1 systematically by ^{59}Co NQR at zero magnetic field, which corresponds to the configuration of $H \parallel c$ axis since the principal axis of the EFG is along the c axis. As shown in Fig. 4, the T dependence of $1/T_1T$ shows systematic change with decreasing Li content, except for CoO_2 which will be discussed separately. With decreasing x from 0.35 to 0.12 , $1/T_1T$ increases as T decreases, indicating that the electron correlations are induced. Also, the increase is more pronounced in samples with smaller x , which indicates that the spin correlation is stronger in samples with smaller x . A similar situation was encountered in $\text{Na}_x\text{CoO}_2 \cdot 1.3\text{H}_2\text{O}$ ($x=0.35, 0.33, 0.28$, and 0.25).³ As in that case, the correlation is antiferromagnetic in origin since the Knight shift is T independent. The $1/T_1T$ becomes constant below T^* , indicating a renormalized Fermi-liquid state below T^* . This situation resembles that in electron-doped cuprate $\text{Pr}_{0.91}\text{LaCe}_{0.09}\text{CuO}_4$ where $T^* \sim 60$ K.¹⁹ Furthermore, T^* systematically decreases from 50 K for $x=0.25$ to 7 K for $x=0.12$. This also indicates that a sample with smaller x is closer to a magnetic instability. Therefore, the results are

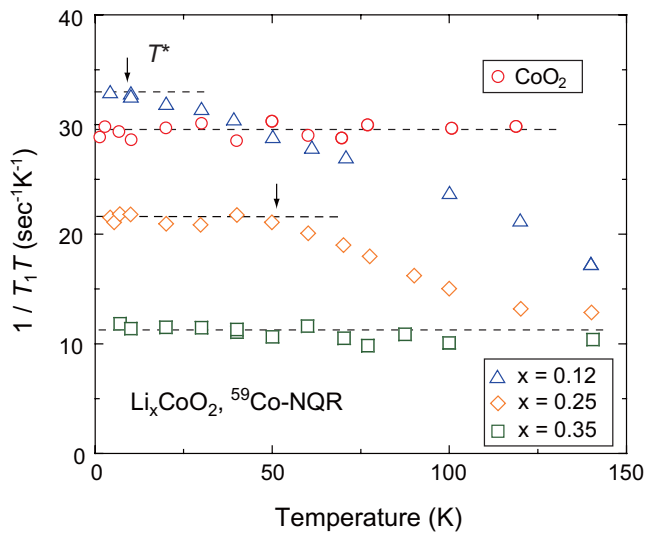


FIG. 4. (Color online) T dependence of $^{59}\text{Co-NQR}1/T_1T$ for Li_xCoO_2 ($x=0.35, 0.25, 0.12$, and 0.0). Dotted lines and arrows indicate the relation of $1/T_1T=\text{constant}$ and T^* , respectively.

consistent with the theories for a compound near a magnetic transition.^{7,8}

However, $1/T_1T$ is constant for CoO_2 . This abrupt change in the electronic state is clearly due to the abrupt change in the crystal structure. The Li_xCoO_2 phase with finite x has a highly two-dimensional crystal structure in which the inter-layer Co-Co distance ($d_{\text{Co-Co}}$) is as large as 5.0–5.1 Å, while CoO_2 crystallizes in a less anisotropic structure. Since there is no “spacer” layer between two adjacent CoO_2 blocks when Li ions are completely extracted, the $d_{\text{Co-Co}}$ value is reduced to 4.24 Å in CoO_2 . The emergent three dimensionality is

believed to be the origin of the weak electron correlation of CoO_2 .

Finally, we examine if there exists any renormalization effect in CoO_2 . To this end, we evaluate the Korringa ratio, $S=T_1TK_s^2 \cdot \frac{4\pi k_B}{h} \left(\frac{\gamma_n}{\gamma_e}\right)^2$. This quantity is unity for a free-electron system. It is much smaller than the unity for an antiferromagnetically correlated metal but much larger than the unity for a ferromagnetically correlated metal.²⁰ In the present case, we use the $K_{\text{orb}}^a=2.96\%$ and $K_{\text{orb}}^c=1.72\%$ obtained from recent NMR study in single-crystalline $\text{Na}_{0.42}\text{CoO}_2$,⁶ and then we obtain $S=1.12 \pm 0.04$ for CoO_2 . Therefore, CoO_2 is a conventional metal that well conforms to Fermi-liquid theory.

In conclusion, we have presented $^{59}\text{Co-NMR}$ and NQR measurements and analysis on Li_xCoO_2 ($x=0.0-0.35$). The antiferromagneticlike spin fluctuations develop when Li is deintercalated from $\text{Li}_{0.35}\text{CoO}_2$, which is consistent with the picture that the member of the families $A_x\text{CoO}_2$ ($A=\text{Li, Na}$) with small x is viewed as a doped spin 1/2 system. Due to the emergent three dimensionality of the crystal structure, however, CoO_2 , the $x=0$ end member of $A_x\text{CoO}_2$, is a conventional metal that well conforms to Fermi-liquid theory. The result highlights the importance of two dimensionality for electron correlations in $A_x\text{CoO}_2$, as was the case that water intercalated into noncorrelated $\text{Na}_{0.42}\text{CoO}_2$ brings about spin fluctuations.⁶ We hope that these results form a foundation for understanding cobalt oxides and the superconductivity developed out of there.

This work was supported in part by research grants from MEXT (Grant No. 17072005) and JSPS, and also by Tekes (Grant No. 1726/31/07) and Academy of Finland (Grant No. 110433).

- ¹K. Takada, H. Sakurai, E. Takayama-Muromachi, F. Izumi, R. A. Dilanian, and T. Sasaki, *Nature* (London) **422**, 53 (2003).
- ²T. Fujimoto, G.-q. Zheng, Y. Kitaoka, R. L. Meng, J. Cmaidalka, and C. W. Chu, *Phys. Rev. Lett.* **92**, 047004 (2004).
- ³G.-q. Zheng, K. Matano, R. L. Meng, J. Cmaidalka, and C. W. Chu, *J. Phys.: Condens. Matter* **18**, L63 (2006).
- ⁴E. Kusano, S. Kawasaki, K. Matano, G.-q. Zheng, R. L. Meng, J. Cmaidalka, and C. W. Chu, *Phys. Rev. B* **76**, 100506(R) (2007).
- ⁵G.-q. Zheng, K. Matano, D. P. Chen, and C. T. Lin, *Phys. Rev. B* **73**, 180503(R) (2006).
- ⁶K. Matano, C. T. Lin, and G.-q. Zheng, *EPL* **84**, 57010 (2008).
- ⁷G. Baskaran, *Phys. Rev. Lett.* **91**, 097003 (2003).
- ⁸Q.-H. Wang, D.-H. Lee, and P. A. Lee, *Phys. Rev. B* **69**, 092504 (2004).
- ⁹M. Ogata, *J. Phys. Soc. Jpn.* **72**, 1839 (2003).
- ¹⁰J. Kunes, K. W. Lee, and W. E. Pickett, in *New Challenges in Superconductivity: Experimental Advances and Emerging Theories*, edited by J. Ashkenazi *et al.* (Kluwer Academic, Boston, 2004), pp. 235–242.
- ¹¹C. de Vaulx, M.-H. Julien, C. Berthier, S. Hebert, V. Pralong, and A. Maignan, *Phys. Rev. Lett.* **98**, 246402 (2007).
- ¹²K. Mukai, Y. Ikedo, H. Nozaki, J. Sugiyama, K. Nishiyama, D. Andreica, A. Amato, P. L. Russo, E. J. Ansaldo, J. H. Brewer, K. H. Chow, K. Ariyoshi, and T. Ohzuku, *Phys. Rev. Lett.* **99**, 087601 (2007).
- ¹³G. G. Amatucci, J.-M. Tarascon, and L. C. Klein, *J. Electrochem. Soc.* **143**, 1114 (1996).
- ¹⁴T. Motohashi, Y. Katsumata, T. Ono, R. Kanno, M. Karppinen, and H. Yamauchi, *Chem. Mater.* **19**, 5063 (2007).
- ¹⁵T. Motohashi, T. Ono, Y. Katsumata, and R. Kanno, *J. Appl. Phys.* **103**, 07C902 (2008).
- ¹⁶A. Narath, *Phys. Rev.* **162**, 320 (1967).
- ¹⁷J. Chepin and J. H. Ross, *J. Phys.: Condens. Matter* **3**, 8103 (1991).
- ¹⁸A. Abragam, *The Principles of Nuclear Magnetism* (Oxford University Press, London, 1961).
- ¹⁹G.-q. Zheng, T. Sato, Y. Kitaoka, M. Fujita, and K. Yamada, *Phys. Rev. Lett.* **90**, 197005 (2003).
- ²⁰T. Moriya, *J. Phys. Soc. Jpn.* **18**, 516 (1963).